

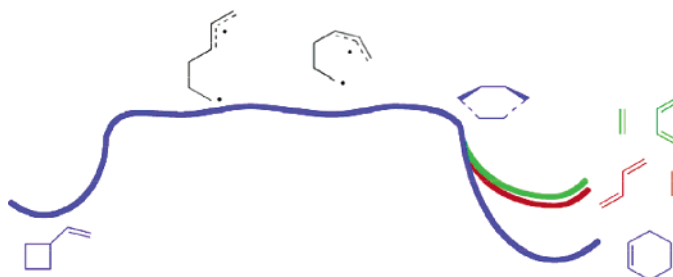
Vinylcyclobutane–Cyclohexene Rearrangement: Theoretical Exploration of Mechanism and Relationship to the Diels–Alder Potential Surface

Brian H. Northrop and K. N. Houk*

Department of Chemistry and Biochemistry, University of California, Los Angeles, California 90095-1569

houk@chem.ucla.edu

Received June 21, 2005



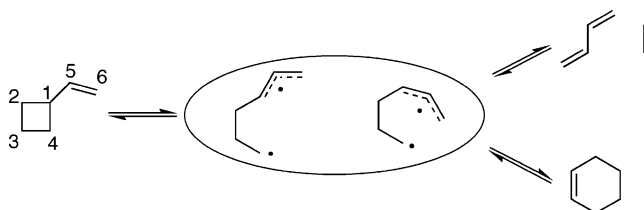
The vinylcyclobutane–cyclohexene rearrangement has been studied computationally with density functional theory and complete active space SCF calculations. The rearrangement proceeds through a diradical that exists on a very flat potential energy surface. Transition structures for conformational processes, only slightly higher in energy than the minimum energy reaction path, account for the stereochemistries of products observed in the thermal rearrangements of vinylcyclobutane derivatives. The connection of this rearrangement to the Diels–Alder reaction of butadiene with ethylene is discussed.

Introduction

Vinylcyclobutane may rearrange thermally to cyclohexene or fragment to butadiene and ethylene via diradical species (Scheme 1). Both *anti* and *syn* conformers exist for vinylcyclobutane: in the former, the vinyl group is *anti* to the cyclobutane ring, whereas in the latter the vinyl group is *syn* to the cyclobutane. Both *cis* and *trans* diradical intermediates are feasible depending on the conformation of the vinylcyclobutane upon carbon–carbon bond cleavage.

The rearrangements of substituted bicyclo[3.2.0]hept-2-enes to norbornene derivatives, examples of the vinylcyclobutane–cyclohexene rearrangement, were reported in 1962 by Berson (Scheme 2a).¹ Ellis and Frey observed the thermal rearrangement of isopropenylcyclobutane to 1-methylcyclohexene in 1963 (Scheme 2b).² The vinylcyclobutane–cyclohexene rearrangement of *syn-cis*-bicyclo[3.2.0]hept-2-enyl-6-acetate was recognized soon thereafter as a potentially concerted [1,3] sigmatropic shift.³

SCHEME 1



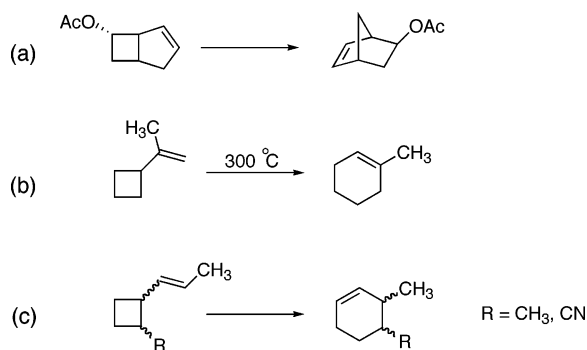
The rearrangement can proceed suprafacially or antarafacially with respect to the allyl moiety and with inversion or retention of configuration at the migrating carbon. These four possibilities are referred to as *si*, *sr*, *ai*, and *ar*. The Woodward–Hoffmann orbital symmetry rules predict that concerted reactions can occur through the *si* and *ar* pathways.³ In the ensuing 40 years, a number of vinylcyclobutane derivatives have been studied, and interesting mechanistic and stereochemical phenomena have been discovered. Prompted by orbital symmetry arguments of

(1) Berson, J. A.; Patton, J. W. *J. Am. Chem. Soc.* **1962**, *84*, 3406–3407.

(2) Ellis, R. J.; Frey, H. M. *Trans. Faraday Soc.* **1963**, *59*, 2076–2079.

(3) Woodward, R. B.; Hoffmann, R. *Angew. Chem., Int. Ed. Engl.* **1969**, *8*, 829–838; see p 829.

SCHEME 2



Woodward and Hoffmann, Berson and Nelson conducted experimental investigations into the stereochemistry of the migrating group in thermal concerted [1,3] sigmatropic rearrangements.⁴ Whereas the predicted [1*i*,3*s*] stereochemistry was found to be favored in some cases, other sterically hindered cases led to a preponderance of the symmetry-forbidden [1*r*,3*s*] pathway. This led to the proposal of “subjacent orbital control” in which the forbidden concerted process was suggested to be preferred over a stepwise process.⁵ Baldwin et al. reviewed the vinylcyclobutane to cyclohexene rearrangement in 2002.^{6b}

Baldwin et al. studied the rearrangements of different 1-(*E*)-propenyl-2-(substituted)-cyclobutanes to *cis*- and *trans*-3-methyl-4-(substituted)-cyclohexenes (Scheme 2c, R = Me).⁶ In 1974 Doering et al. studied the thermal rearrangements of *cis*- and *trans*-1-cyano-2-isopropenylcyclopropane and concluded that the transition state was best described as a “continuous diradical”.^{7a} Shortly thereafter and as recently as 2002, Doering investigated the applicability of orbital symmetry rules to the “not obviously concerted” rearrangement of 1-cyano-2-vinylcyclobutane to 4-cyanocyclohexene, as well as *cis*- and *trans*-1-cyano-2-*trans*-propenylcyclobutane to 4-cyano-3-methylcyclohexenes (Scheme 2c, R = CN).^{7b,c}

Typical product distributions for vinylcyclobutane rearrangements of 1-(*E*)-propenyl-2-(substituted)-cyclobutanes^{6a,7c,8b} and for bicyclic versions studied by Berson^{4c} are shown in Table 1. Although a mixture of all possible stereochemistries is obtained, product distributions are not random and often show a preference for the Woodward–Hoffmann allowed products. Even so, small changes in the vinylcyclobutane derivative can drastically affect the preference for “allowed” or “forbidden” products. For example, while *trans*-1-propenyl-2-methylcyclobutane shows a small preference for the “allowed” products with a (*si*+*ar*)/(*sr*+*ai*) ratio of 1.7 (Table 1, entry c), the *cis* isomer shows a small preference for the “forbidden” products with a ratio of 0.4 (Table 1, entry d). This follows the pattern discussed by Berson and Nelson, where even higher stereoselectivity was

observed. Berson and Nelson noted a dramatic change in preference for inversion or retention between 7-*exo*-methyl- and 7-*endo*-methyl-substituted 6-endo-acetoxycyclo[3.2.0]hept-2-enes. Whereas the 7-*exo*-methyl system showed a preference for inversion with a (*si*/*sr*) ratio of 9.3, the 7-*endo*-methyl system proceeds with retention and a (*si*/*sr*) ratio of 0.14 (Table 1, entries g and h).^{4c}

Studies by Berson,⁸ Baldwin,⁶ and Doering⁷ of thermal [1,3] sigmatropic rearrangements of vinylcyclobutanes have provided much insight into the mechanism. The potential energy surface of the vinylcyclobutane rearrangement can be described as a caldera,⁹ as it is very flat, without well-defined minima, and characterized by easy rotation about single bonds. The dynamics of these rotations ultimately determine the stereochemistry of the resulting cyclohexene derivative.

The vinylcyclopropane to cyclopentene rearrangement is another example of a [1,3] sigmatropic shift that has been shown to proceed via diradical intermediates.¹⁰ In 2003 Baldwin reviewed the stereochemistry, kinetics, substituent effects, dynamics, and computational investigations of the vinylcyclopropane rearrangement.^{10c} All four possible product stereochemistries may also be obtained for this rearrangement. Product distributions, as calculated by deuterium labeling, are *si* = 40%, *sr* = 23%, *ar* = 13%, and *ai* = 24%.^{10b} No substantial preference for the orbital-symmetry-allowed products was observed. Overall, experimental results have shown that relative ratios of product stereochemistries can be influenced by the flexibility of the vinyl group, whether the molecule is monocyclic or bicyclic, the stereochemistry of the substituent(s) α to the migrating carbon, and the size of the substituent(s) on the migrating carbon.^{6b}

Theoretical studies of [1,3] sigmatropic shifts have provided valuable information about the transition structures of these processes.¹¹ Beno et al. and Wilsey et al. have studied computationally the rearrangements of bicyclo[3.2.0]hept-2-enes to norbornenes.¹² Carpenter’s dynamics calculations indicate that the preference for inversion of configuration in [1,3] shifts of 1-phenylbicyclo[2.1.1]hexane and bicyclo[3.2.0]hept-2-ene result from the dynamical effects in the ring-cleavage transition state.¹³ Davidson and Gajewski^{14a} and Houk et al.^{14b–d} have studied the rearrangement of vinylcyclopropane to cyclopentene, whereas Doubleday^{14b,15} has used quasiclassical direct dynamics to investigate the rearrangement mechanism. In 2002 Suhrada and Houk studied the quadruply degenerate rearrangement of bicyclo[3.1.0]hex-2-ene, a bicyclic vinylcyclopropane rearrange-

(9) Doering, W. v. E.; Eklmanis, J. L.; Belfield, K. D.; Klärner, F.-G.; Krawczyk, B. *J. Am. Chem. Soc.* **2001**, *123*, 5532–5541.

(10) (a) Frey, H. M.; Walsh, R. *Chem. Rev.* **1969**, *8*, 781–853. (b) Baldwin, J. E.; Villarica, K. A.; Freedberg, D. I.; Anet, F. A. L. *J. Am. Chem. Soc.* **1994**, *116*, 10845–10846. (c) Baldwin, J. E. *Chem. Rev.* **2003**, *103*, 1197–1212.

(11) Wiest, O.; Montiel, D. C.; Houk, K. N. *J. Phys. Chem.* **1997**, *101*, 8378–8388.

(12) (a) Beno, B. R.; Wilsey, S.; Houk, K. K. *J. Am. Chem. Soc.* **1999**, *121*, 4816–4826. (b) Wilsey, S.; Houk, K. N.; Zewail, A. H. *J. Am. Chem. Soc.* **1999**, *121*, 5772–5786.

(13) (a) Carpenter, B. K. *J. Org. Chem.* **1992**, *57*, 4645–4648. (b) Carpenter, B. K. *J. Am. Chem. Soc.* **1995**, *117*, 6336–6344. (c) Carpenter, B. K. *Angew. Chem., Int. Ed.* **1998**, *37*, 3340–3350.

(14) (a) Davidson, E. R.; Gajewski, J. J. *J. Am. Chem. Soc.* **1997**, *119*, 10543–10544. (b) Houk, K. N.; Nendel, M.; Wiest, O.; Storer, J. W. *J. Am. Chem. Soc.* **1997**, *119*, 10545–10546. (c) Doubleday, C.; Nendel, M.; Houk, K. N.; Thweatt, D.; Page, M. *J. Am. Chem. Soc.* **1999**, *121*, 4720–4721. (d) Nendel, M.; Sperling, D.; Wiest, O.; Houk, K. N. *J. Org. Chem.* **2000**, *65*, 3259–3268.

(15) Doubleday, C. *J. Phys. Chem. A* **2001**, *105*, 6333–6341.

(4) (a) Berson, J. A.; Nelson, G. L. *J. Am. Chem. Soc.* **1967**, *89*, 5503–5504. (b) Berson, J. A. *Acc. Chem. Res.* **1968**, *1*, 152–160. (c) Berson, J. A.; Nelson, G. L. *J. Am. Chem. Soc.* **1970**, *92*, 1096–1097.

(5) Berson, J. A.; Salem, L. *J. Am. Chem. Soc.* **1972**, *94*, 8917–8918.

(6) (a) Baldwin, J. E.; Burrell, R. C. *J. Am. Chem. Soc.* **2001**, *123*, 6718–6719. (b) Leber, P. A.; Baldwin, J. E. *Acc. Chem. Res.* **2002**, *35*, 279–287 and references therein. (c) Baldwin, J. E.; Burrell, R. C. *J. Am. Chem. Soc.* **2003**, *125*, 15869–15877.

(7) (a) Doering, W. v. E.; Sachdev, K. *J. Am. Chem. Soc.* **1974**, *96*, 1168–1187. (b) Doering, W. v. E.; Mastrocola, A. R. *Tetrahedron* **1981**, *37* (Suppl. 1), 329–334. (c) Doering, W. v. E.; Cheng, X.; Lee, W.; Lin, Z. *J. Am. Chem. Soc.* **2002**, *124*, 11642–11652.

(8) (a) Berson, J. A.; Dervan, P. B. *J. Am. Chem. Soc.* **1973**, *95*, 267–269. (b) Berson, J. A.; Dervan, P. B. *J. Am. Chem. Soc.* **1973**, *95*, 269–270.

TABLE 1. Product Distributions and Woodward–Hoffmann “Allowed” vs “Forbidden” Ratios for Rearrangements of a Variety of 1-(*E*)-Propenyl-2-(substituted)-cyclobutanes to *cis*- and *trans*-3-Methyl-4-(substituted)-cyclohexenes^{6a,7,8b} and Both 7-*exo*-Methyl- and 7-*endo*-Methyl-Substituted 6-endoacetoxybicyclo[3.2.0]hept-2-enes^{4c}

		W.-H. Allowed		W.-H. Forbidden		$(si+ar)/(sr+ai)$	ref.
		<i>si</i>	<i>ar</i>	<i>sr</i>	<i>ai</i>		
a)		49 %	3 %	48 %	0 %	1.1	8b
b)		50 %	6 %	41 %	3 %	1.3	8b
c)		58 %	5 %	33 %	4 %	1.7	6a
d)		18 %	11 %	51 %	20 %	0.4	6a
e)		48 %	20 %	27 %	6 %	2.1	7c
f)		13 %	5 %	66 %	16 %	0.2	7c
g)		$(si/sr) > 9.3$					4c
h)		$(si/sr) < 0.14$					4c

ment.¹⁶ Results of these computational studies are consistent with the model that product stereochemistries of rearrangements of this type are determined by the dynamics of diradical species that exist on flat potential surfaces. There have been suggestions of some control of their motions by orbital interactions.^{14b}

We have performed a theoretical investigation of the rearrangement of vinylcyclobutane to cyclohexene. Computational methods that have proven robust for related hydrocarbon rearrangements through diradicals were employed. The mechanism of this rearrangement has been shown to proceed via diradical intermediates and to include two distinct processes: (1) the cyclobutane ring opening to form the diradical and (2) ring closure to form cyclohexene or cleavage to butadiene plus ethylene. Geometries and energies of stationary points on the ring-closing portion of the vinylcyclobutane potential energy surface show that the rearrangement may merge with the stepwise butadiene plus ethylene Diels–Alder reaction mechanism that has been studied extensively.¹⁷ The most energetically favored pathway is suprafacial with inversion, but deviations from this pathway through stationary points only slightly higher in energy lead to the three other products.

Computational Methodology

The potential surfaces for fragmentation and rearrangement were explored by scanning bond lengths and bond rotations in order to locate stationary points. Stationary points on the vinylcyclobutane–cyclohexene potential surface were optimized at the UB3LYP/6-31G* and CASSCF(6,6)/6-31G* levels. Single point energies were also computed at the CASPT2(6,6)/6-31G*//UB3LYP/6-31G* level. These calculations have been found to be reliable for a variety of similar hydrocarbon diradical species.^{11,16,18} UB3LYP/6-31G* and CASSCF(6,6)/6-31G* calculations were performed using GAUSSIAN98,¹⁹ and CASPT2(6,6)/6-31G* single point calculations were performed using MOLCAS.²⁰ Closed-shell wave functions were

(17) (a) Li, Y.; Houk, K. N. *J. Am. Chem. Soc.* **1993**, *115*, 7478–7485. (b) Houk, K. N.; Li, Y.; Storer, J.; Raimond, L.; Beno, B. *J. Chem. Soc., Faraday Trans.* **1994**, *90*, 1549–1604. (c) Jursic, B.; Zdraukovshii, Z. *J. Chem. Soc., Perkin Trans. 2* **1995**, *6*, 1223–1226. (d) Goldstein, E.; Beno, B.; Houk, K. N. *J. Am. Chem. Soc.* **1996**, *118*, 6036–6043. (e) Bradley, A. Z.; Kocielek, M. G.; Johnson, R. P. *J. Org. Chem.* **2000**, *65*, 7134–7138. (f) Kobko, N.; Dannenberg, J. J. *J. Phys. Chem. A* **2001**, *105*, 1944–1950. (g) Kraka, E.; Wu, A.; Cremer, D. *J. Phys. Chem. A* **2003**, *107*, 9008–9021.

(18) (a) Leach, A. G.; Houk, K. N. *J. Am. Chem. Soc.* **2002**, *124*, 14820–14821. (b) Leach, A. G.; Goldstein, E.; Houk, K. N. *J. Am. Chem. Soc.* **2003**, *125*, 8330–8339.

(19) *Gaussian 98*, revision A.9; Frisch, M. J. et. al.; Gaussian, Inc.: Pittsburgh, PA, 1998.

(20) *MOLCAS*, Version 5.0; Anderson, K. et. al.; Lund University: Lund, Sweden, 2001.

(16) Suhrada, C. P.; Houk, K. N. *J. Am. Chem. Soc.* **2002**, *124*, 8796–8797.

TABLE 2. Summary of Calculated Energies of Stationary Points Found for Fragmentation and Rearrangement of Vinylcyclobutane^a

molecule	UB3LYP		CASSCF	CASPT2
	E _{rel}	E _{rel} (spin corrected)	E _{rel}	E _{rel}
<i>anti</i> -vinylcyclobutane (1)	0.0	0.0	0.0	0.0
<i>trans-endo</i> ring opening T.S. (2)	42.6	37.7	38.0	43.5
<i>trans-exo</i> ring opening T.S. (2')	44.4	39.6	49.9	44.1
<i>trans-gauche</i> diradical int (3)	39.7	33.2	37.1	44.4
2,3-rotation T.S. (4)	42.9	41.1	40.2	46.1
<i>trans-anti</i> diradical int. (5)	39.3	40.5	36.7	42.5
fragmentation T.S. (6)	44.1	38.6	40.6	46.0
butadiene + ethylene (7)	1.6	1.6	9.0	6.1
<i>anti-syn</i> T.S. (8)	2.9	2.9	0.3	2.3
<i>syn</i> -vinylcyclobutane (9)	0.9	0.9	-4.5	0.5
<i>cis-endo</i> ring opening T.S. (10)	43.2	38.4	37.4	44.1
<i>cis-exo</i> ring opening T.S. (10')	45.0	40.2	50.9	44.4
<i>cis</i> -diradical int. (11)	41.1	40.2	37.8	45.6
2,3-rotation/closure T.S. (12)	43.9	41.8	52.2	48.1
concerted T.S. (13)	38.0	38.0	43.3	42.2
cyclohexene (14)	-22.9	-22.9	-22.5	-24.1
3,4-rotation T.S. (15)	41.3	41.4	35.2	46.6
2,3-rotation T.S. (16)	43.8	43.1	41.6	49.1
<i>gauche-out</i> diradical int (17)	41.6	41.0	38.6	46.2
<i>cis</i> -fragmentation T.S. (18)	47.2	41.8	44.3	49.2
<i>cis</i> -butadiene + ethylene (19)	5.5	5.5	27.9	9.7

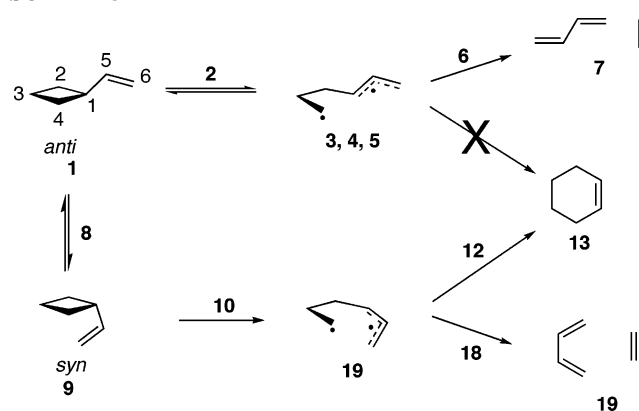
^a Energies are relative to *anti*-vinylcyclobutane (1) and are in kcal/mol. All UB3LYP/6-31G* and CASSCF(6,6)/6-31G* structures were optimized at that level. CASPT2(6,6)/6-31G* single points were performed using UB3LYP/6-31G* optimized geometries and zero point corrections.

most stable for reactants and products, and open-shell wave functions were obtained for all transition states and diradical species. Zero point and free energy corrections were made for UB3LYP/6-31G* and CASSCF(6,6)/6-31G* optimized structures with frequency calculations. CASPT2(6,6)/6-31G* single points were zero point and thermally corrected with UB3LYP/6-31G* zero point and free energies. Vibrational frequency calculations were carried out on all stationary points to distinguish transition states from reactants, intermediates, and products. Transition states were identified as having one imaginary frequency, while all reactants, intermediates, and products had none.

Calculated UB3LYP/6-31G* wave functions exhibited varying degrees of spin contamination, and $\langle S^2 \rangle$ values for singlet diradical species ranged from 0.6 to 1.03. Triplet energies of singlet diradical species were calculated and used to correct for spin contamination using the spin correction method developed by Yamaguchi et al.²¹ Both spin-corrected and spin-contaminated UB3LYP/6-31G* energies are reported.

Results and Discussion

UB3LYP/6-31G*, CASSCF(6,6)/6-31G*, and CASPT2(6,6)/6-31G*//UB3LYP/6-31G* energies of all stationary points found are listed in Table 2. Vinylcyclobutane may exist in either the *anti* or *syn* conformation as shown in Scheme 3. The *anti* conformer is 0.9 kcal/mol more stable according to UB3LYP/6-31G* but is in rapid equilibrium with the *syn* isomer. The barrier between the two is calculated to be only 2.9 kcal/mol, corresponding to a rate of interconversion on the order of 10^{11} s⁻¹. Optimized structures of stationary points located on the *anti* surface are shown in Figure 1, and relative energies of these structures are shown in Figure 2. Opening of the cyclobutane

SCHEME 3

ring of *anti*-vinylcyclobutane forms a *trans*-diradical. The ring-opening transition state 2 initiates rotation of the methylene group. If the cleavage occurs in a linear fashion, an unfavorable, four-electron, antiaromatic interaction develops between the breaking σ bond and the vinyl π system.^{14a} To avoid this interaction, the developing methylene group rotates so as to reduce overlap of the p orbital and the π system of the developing allylic radical in the ring-opening transition state, as shown in structure 2. This rotation of C4, where rotation away from the developing allylic radical has been termed “endo”, reduces overlap of the primary radical with the two termini of the allyl radical. An alternative, “exo”, ring-opening transition state is also possible (2'). The exo transition state is characterized by C3–C4 bond rotation in such a way that the p orbital on C4 is directed toward the π system and increases overlap with the developing allylic radical. This unfavorable interaction causes the exo transition state to be 1.9 kcal/mol higher energy than the endo transition state as calculated with UB3LYP/6-31G*. Doubleday has found that the cyclization of tetramethylene, the reverse path of cyclobutane ring opening, occurs with rotation of one methylene in order to avoid this antiaromatic interaction.²² The related methylene rotation in vinylcyclobutane can be seen in formation of *trans-gauche* diradical intermediate 3. Intermediate 3 differs from opening transition state 2 primarily by 102° of rotation around the C4–C3 bond, and 3 is found to be 4.5 kcal/mol lower in energy than 2 on the UB3LYP/6-31G* surface. With CASSCF/6-31G* this drops to 0.9 kcal/mol, while the minimum no longer exists with CASPT2/6-31G*//UB3LYP/6-31G*.

Closure of the *trans*-diradical to *cis*-cyclohexene would require an energetically unfavorable rotation around the C1–C5 bond of the allylic radical, with an activation barrier of around 15 kcal/mol.^{14c} Johnson et al. have studied the formation of *trans*-cyclohexene from *trans*-butadiene and ethylene with a variety of computational methods.^{17e} While it was concluded that *trans*-cyclohexene may play a role in the Diels–Alder cycloreversion of *cis*-cyclohexene, its formation from a *trans*-diradical was shown to be highly unlikely given that the diradical transition state leading to the formation of *trans*-cyclohexene from a *trans*-diradical was shown to be 10–13 kcal/mol higher energy than that of fragmentation at the UB3LYP/6-31G* level. Neither stereochemistry nor the relationship to the vinylcyclobutane surface were studied. Therefore, reclosure to reform vinylcyclobutane or fragmentation to 1,3-butadiene and ethylene

(21) (a) Yamaguchi, K.; Jensen, F.; Dorigo, A.; Houk, K. N. *Chem. Phys. Lett.* **1998**, *149*, 537. (b) Yamaguchi, K.; Kawakami, T.; Nagao, H.; Yamaguchi, K. *Chem. Phys. Lett.* **1994**, *231*, 25.

(22) (a) Doubleday, C. *Chem. Phys. Lett.* **1995**, *233*, 509–513. (b) Doubleday, C. *J. Phys. Chem.* **1996**, *100*, 15083–15086.

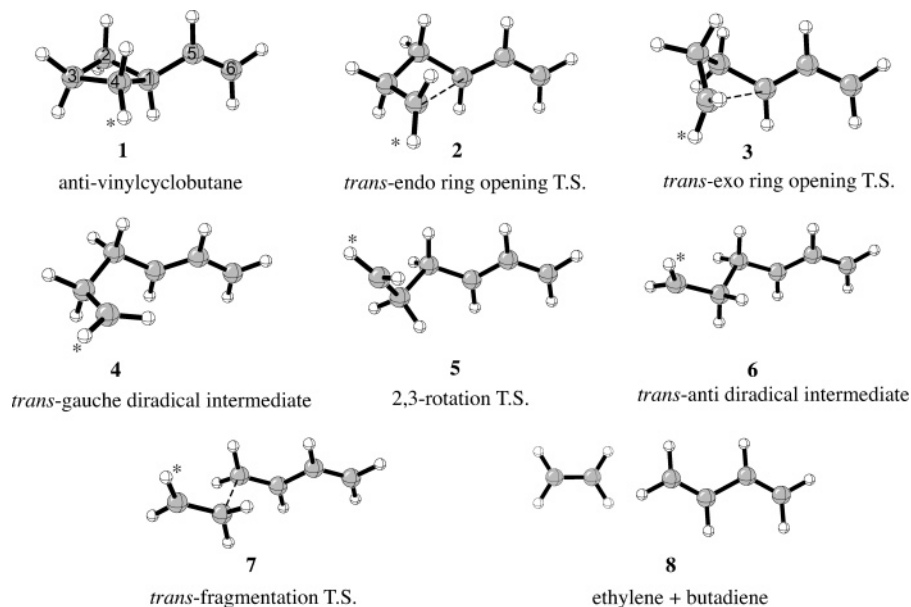


FIGURE 1. UB3LYP/6-31G* and CASSCF(6,6)/6-31G* geometry optimized stationary points along the pathway for fragmentation of *anti*-vinylcyclobutane to ethylene and 1,3-butadiene. One of the hydrogens at C4 is marked with an asterisk to follow consequences of rotations along the reaction path. Dashed lines indicate bonds being broken.

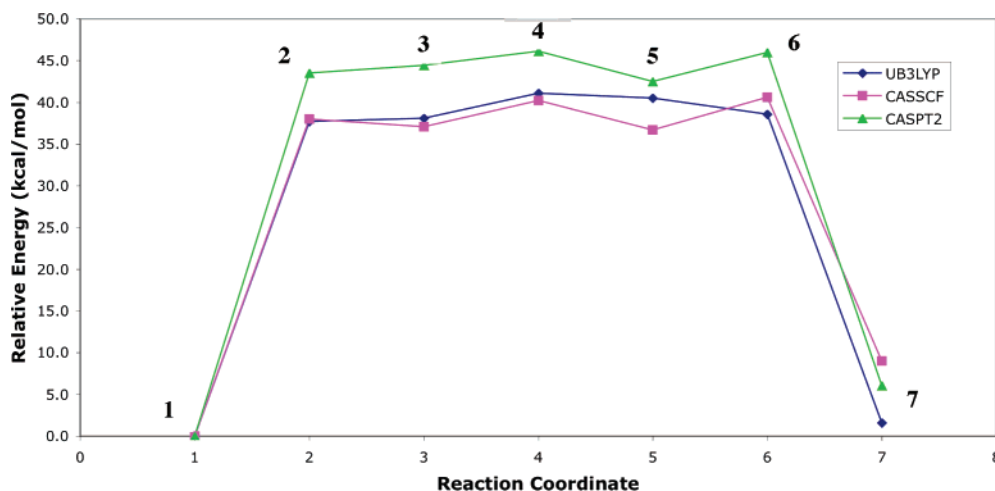


FIGURE 2. Relative energies of stationary points on the vinylcyclobutane fragmentation pathway.

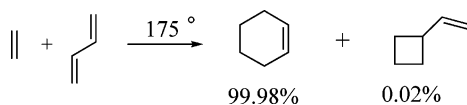
are the only two energetically feasible pathways available for the *trans* diradical. Five stationary points were found to lie on the minimum energy pathway between *anti*-vinylcyclobutane **1** and butadiene plus ethylene **7**; these are ring-opening transition state **2**, *trans*-gauche diradical intermediate **3**, 2,3-rotation transition state **4**, *trans-anti* diradical intermediate **5**, and fragmentation transition state **6**. $\langle S^2 \rangle$ values for singlet diradical species **2–6** ranged from 0.60 to 1.02 with UB3LYP/6-31G*. Stationary points **3** and **6** have nearly the same geometries and energies as those found by Johnson et al. in their study of the Diels–Alder cycloaddition of ethylene and *trans*-1,3-butadiene.^{17c}

For fragmentation to butadiene and ethylene to occur, the radical centers must be aligned with the C2–C3 bond. This is not the case in *trans*-gauche diradical intermediate **3**. Transition state **4**, which corresponds to rotation around the C2–C3 bond, is 3.0 kcal/mol higher in energy than gauche intermediate **3** and connects intermediate **3** with the *trans-anti* diradical intermediate **5**. After spin correction, intermediate **5** is only 0.6 kcal/mol more stable than transition state **4** by UB3LYP/6-31G*,

while CASPT2(6,6)/6-31G**/UB3LYP/6-31G* calculations predict **5** to be 3.6 kcal/mol lower than **4**. In intermediate **5**, radical centers are in the proper alignment for fragmentation, which occurs through fragmentation transition state **6**. The rotation around the C3–C4 bond that occurs on the lowest energy pathway for fragmentation converts *cis* substituents on carbons 3 and 4 in vinylcyclobutane to *trans* in the resulting ethylene and vice versa. Fragmentation is calculated to be overall endothermic by 1.6 kcal/mol but is entropically favored and can occur at high temperature. Whereas UB3LYP/6-31G* calculations predict the rate determining step for fragmentation to be 2,3-rotation transition state **4**, CASSCF(6,6)/6-31G* calculations predict fragmentation transition state **6** to be 0.4 kcal/mol higher in energy than 2,3-rotation transition state **4**. CASPT2(6,6)/6-31G**/UB3LYP/6-31G* single point calculations also predict the reaction to be endothermic (6.1 kcal/mol); however, this level of theory predicts 2,3-rotation transition state **4** and fragmentation transition state **6** to be of near equal energy, 46.1 and 46.0 kcal/mol, respectively. Only one energetic

TABLE 3. Comparison of Calculated and Experimental Activation Energies (kcal/mol) and Reaction Enthalpies for Fragmentation and Rearrangement of Vinylcyclobutane

	UB3LYP	CASSCF	CASPT2	exptl
ΔH^\ddagger fragmentation	41.1	40.6	46.1	49.8 \pm 0.4
ΔH_f° fragmentation	1.6	9.0	6.1	14.8 \pm 0.6
ΔH^\ddagger rearrangement	41.8	52.2	48.1	47.5 \pm 0.5
ΔH_f° rearrangement	-22.9	-22.5	-24.1	-24.9

SCHEME 4

minimum exists on the CASPT2(6,6)/6-31G**/UB3LYP/6-31G* potential surface, that of the *trans-anti* diradical intermediate (**5**). The five stationary points on the CASPT2(6,6)/6-31G**/UB3LYP/6-31G* fragmentation surface all lie within 3.6 kcal/mol of each other, demonstrating how flat the diradical surface is.

Experimental gas-phase ΔH_f° values for vinylcyclobutane, ethylene, and butadiene show the fragmentation pathway to be endothermic by 14.8 \pm 0.6 kcal/mol.²³ UB3LYP/6-31G* calculations underestimate this value by 13.2 kcal/mol and CASPT2(6,6)/6-31G**/UB3LYP/6-31G* calculations underestimate it by 8.7 kcal/mol. CASSCF(6,6)/6-31G* calculations are closest to experiment and predict the fragmentation to be endothermic by 9.0 kcal/mol (Table 3). The poor ability of such high levels of theory as CASPT2 to predict ΔH_f° of fragmentation is likely due to the fact that the active space of vinylcyclobutane is (6,6) and involves one π orbital and two σ orbitals. Fragmentation products butadiene and ethylene, on the other hand, have active spaces of (4,4) and (2,2), respectively, that involve only π orbitals. CBS-QB3, a high accuracy method generally found to give heats of atomization within 1 kcal/mol of experiment, was used to predict ΔH_f° of vinylcyclobutane fragmentation. Results of the CBS-QB3 calculations show fragmentation to be endothermic by 15.7 kcal/mol, which is in excellent agreement with the experimental value. Additionally, computational predictions of ΔH_f° of rearrangement, where vinylcyclobutane and cyclohexene have the same active space, are in very good agreement with experiment. In 1968, Bartlett et al. observed 0.02% yield of vinylcyclobutane resulting from what is believed to be the [2 + 2] stepwise diradical cycloaddition of ethylene to butadiene (Scheme 4).^{24a} This yield increased to 2.3% when 1,1-dichloro-2,2-difluoroethene was used instead of ethylene.^{24b} These experimentally observed [2 + 2] cycloadditions are the reverse process of vinylcyclobutane fragmentation that has been explored here computationally.

syn-Vinylcyclobutane can rearrange to cyclohexene via a *cis*-diradical. Optimized structures of stationary points located on the *syn* surface are shown in Figure 3, and relative energies of these structures are shown in Figure 4. Three stationary points have been found along the minimum energy pathway. All of these are diradical in nature with singlet (S^2) values between 0.83 and 1.03 from UB3LYP calculations. Two transition states, one ring-opening (**10**) and a 2,3-rotation/closing transition state

(**12**), as well as a *cis*-diradical intermediate (**11**) were found. Two additional transition states, 3,4-rotation transition state **15** and 2,3-rotation transition state **16**, were also located. These transition states are responsible for scrambling the stereochemistry at C4 and will be discussed later.

As was the case in the ring opening of *anti*-vinylcyclobutane, an unfavorable antiaromatic orbital interaction develops as the C1–C4 bond breaks in the opening transition state of *syn*-vinylcyclobutane. This causes the methylene group hybrid orbital to twist away from the π system of the developing allylic radical, leading to the favored endo transition state. This interaction and subsequent orbital rotation is similar to those that govern the stereoselectivity of ring-opening transition states of substituted vinylcyclobutenes (Figure 5). The preference for outward rotation of the vinyl group has been studied by Houk et al. and is an example of torquoselectivity.²⁵ The electron-rich vinyl group in vinylcyclobutene or vinylcyclobutane twists “outward” to avoid unfavorable interactions with the filled HOMO of the breaking σ bond in the transition state. The same sort of interaction occurs in the cleavage of the σ bond of vinylcyclobutane. As with *anti*-vinylcyclobutane, an *exo* ring-opening transition state (**10**) is also possible. This transition state, however, is 1.8 kcal/mol higher in energy than the endo transition state as a result of unfavorable orbital overlap between the p orbital of C4 and the π system of the developing allylic radical as calculated with UB3LYP/6-31G*.

The only intermediate along the lowest energy rearrangement pathway, **11**, is 1.8 kcal/mol higher in energy than ring-opening transition state **10** as calculated with UB3LYP/6-31G*. This value drops slightly to 1.5 kcal/mol with CASPT2(6,6)/6-31G**/UB3LYP/6-31G*. All reported energies that follow are CASPT2(6,6)/6-31G**/UB3LYP/6-31G* unless otherwise noted. It has been observed, therefore, that there exists one stable intermediate, but no energetic minimum, along the lowest energy pathway for rearrangement of *syn*-vinylcyclobutane to cyclohexene. Intermediate **11** differs from transition state **10** primarily by an increased C1–C4 bond distance as well as C2–C3 and C3–C4 bond rotations of 17° and 46°, respectively. The C3–C4 rotation is especially important, because it is this rotation that results in an inversion of stereochemistry at C4 before closure and indicates that the lowest energy pathway is suprafacial with inversion (*si*).

As the methylene radical center approaches the unsubstituted terminus of the allylic radical, the potential energy surface of the vinylcyclobutane–cyclohexene rearrangement may merge with that of the butadiene plus ethylene Diels–Alder reaction.¹⁷ Previous theoretical studies of the stepwise ethylene plus butadiene Diels–Alder reaction located intermediates with nearly the same geometries and energies as diradical intermediate **11** of this study.^{17d,e} Furthermore, it was observed that the C2–C3 bond length of the 2,3-rotation/closing transition state **12** is 0.051–0.073 Å longer than in structures **10**, **11**, and **15**. This indicates that as the C4–C6 bond shortens, there is an elongation of the C2–C3 bond and suggests that the pathway leading from transition state **12** to cyclohexene may intersect with the Diels–Alder concerted transition state **13**. Two vibrational modes of concerted transition state **13** also support this. The first real vibrational mode of **13** corresponds to C2–C3 bond rotation, and the fifth real vibrational mode involves

(23) National Institute of Standards and Technology Database. <http://webbook.nist.gov/chemistry/> (accessed August 2003).

(24) (a) Bartlett, P. D.; Schueller, K. E. *J. Am. Chem. Soc.* **1968**, *90*, 6071–6077. (b) Swenton, S. J.; Bartlett, P. D. *J. Am. Chem. Soc.* **1968**, *90*, 256–258.

(25) (a) Buda, A. B.; Wang, Y.; Houk, K. N. *J. Org. Chem.* **1989**, *54*, 2264–2266. (b) Dolbier, W. R., Jr.; Koroniak, H.; Houk, K. N.; Sheu, C. *Acc. Chem. Res.* **1996**, *29*, 471.

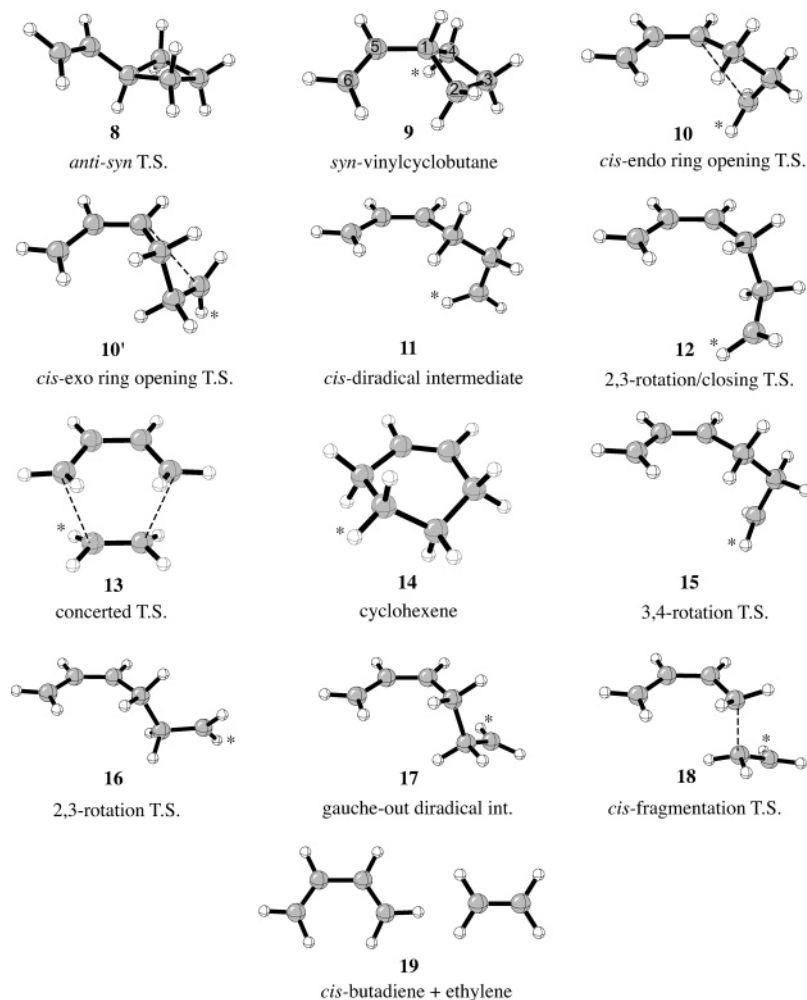


FIGURE 3. UB3LYP/6-31G* and CASSCF(6,6)/6-31G* geometry optimized stationary points along the *si*, *sr*, *ar*, and fragmentation pathways for rearrangement of *syn*-vinylcyclobutane to cyclohexene. Hydrogens at C4 are distinguished with an asterisk to differentiate inversion and retention at C4. Dashed lines indicate the breaking (**10**, **10'**, **18**) or formation (**13**) of covalent bonds.

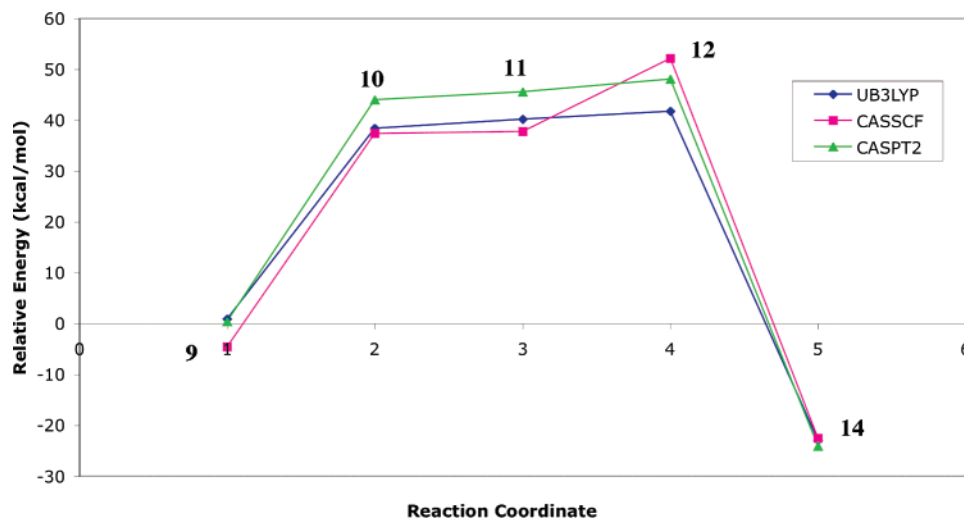


FIGURE 4. Relative energies of stationary points on the *si* rearrangement of *syn*-vinylcyclobutane.

the shortening of one of the forming C–C bonds and the simultaneous lengthening of the other. These two vibrational modes may connect concerted transition state **13** with 2,3-rotation/closing transition state **12**. It should be noted, however, that the pathway from closing transition state **12** to cyclohexene

is entirely downhill in energy, and closure to form cyclohexene from transition state **12** presumably does not exclusively require passage through concerted transition state **13**.

Before closure to cyclohexene through transition state **12**, there exists the possibility of stereochemical scrambling at C4

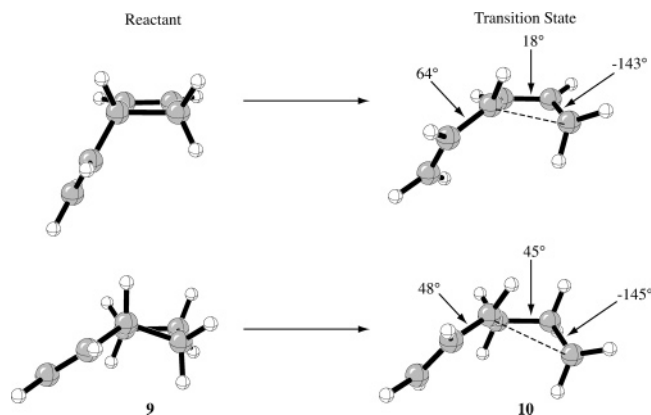


FIGURE 5. Comparison of orbital interactions of vinylcyclobutene and vinylcyclobutane ring-opening transition states. Dihedral angles of relevant torsions are indicated. Dashed lines indicate bonds being broken.

via transition state **15**. Transition state **15** lies only 1.0 kcal/mol higher in energy than intermediate **11**, and the imaginary frequency associated with **15** corresponds to rotation around the C3–C4 bond. It is this rotation that ultimately determines whether the rearrangement proceeds suprafacially with inversion or retention. There is little or no energetic preference for the formation of the Woodward–Hoffmann allowed *si* product over the forbidden *sr* product; the 3,4-rotation transition state, **15**, is 1.0 kcal/mol lower in energy than the 2,3-rotation/closing transition state **12**. However, if the rearrangement proceeds via the *si* pathway (**9-10-11-12-14**), a continuous C3–C4 rotation in one direction is observed. The *sr* pathway (**9-10-11-15-12-14**), however, requires a reversal of C3–C4 rotational momentum in going from intermediate **11** to transition state **15**. While a thorough understanding of bond rotations along the potential surface will require a dynamics simulation, it can be assumed that this reversal of momentum is disfavored relative to the *si* pathway. Doering has noted that the greater the number of internal rotations required of a diradical before it reaches an exit pathway from the potential surface, the longer the lifetime of the diradical, and the smaller its contribution to the stereochemical distribution of products.^{7c}

The reaction coordinate is plotted in Figure 6 as a function of the breaking vinylcyclobutane bond length (*x* axis) and the forming cyclohexene bond length (*y* axis). The rearrangement proceeds via two distinct processes: breaking of the C1–C4 bond that corresponds to horizontal motion in Figure 6, and subsequent C4–C6 bond formation that corresponds to vertical motion. The structural similarity of *cis*-diradical intermediate **11** and 3,4-rotation transition state **15** can also be seen in Figure 6; these have almost identical C1–C4 and C4–C6 bond lengths. Close examination of all stationary points on the *si* pathway shows that after the C1–C4 bond breaks to form the diradical, the terminal methylene group swings out and away from the allylic radical moiety to allow rotation of the C3–C4 bond, as can be seen in intermediate **11**. This conformation requires the greatest separation of carbons 1 and 6, which are those that will form the new cyclohexene bond. As C3–C4 bond rotation proceeds, the p orbital of the methylene carbon orients itself in a way that favors overlap with the allylic radical at carbons 1, 5, and 6. Once this overlap becomes possible, the C4–C6 distance continuously shortens, and the molecule cyclizes through closure transition state **12** to become cyclohexene, **14**. The potential merging of the vinylcyclobutane rearrangement

potential energy surface with that of the Diels–Alder reaction can also be seen from Figure 6. The C1–4 and C4–C6 bond lengths of the concerted transition state of butadiene and ethylene, **13**, fall directly on the reaction coordinate of the breaking vinylcyclobutane and forming cyclohexene bond lengths. Lewis and Baldwin have shown experimentally that heating *cis*-4,5-*d*₂-cyclohexene in a shock tube results in the formation of both *cis*- and *trans*-1,2-*d*₂-ethylene, evidence indicating 1-vinyltrimethylene diradicals and vinylcyclobutane intermediates in the retro Diels–Alder reaction.²⁶

The second most favored pathway for the vinylcyclobutane rearrangement is antarafacial with retention of configuration. Figure 7 shows the energies of structures necessary to achieve the transformation. Rearrangement via the *ar* pathway starts by following the lowest energy pathway through transition state **10** and intermediate **11**. In going from diradical intermediate **11** to closing transition state **12** on the *si* pathway, the C2–C3 bond rotates to bring the terminal methylene closer to the allylic radical, and closure occurs through the butadiene plus ethylene concerted transition state. There exists, however, another transition state that is only 1.0 kcal/mol higher in energy than **12**. This transition state, **16**, takes the rearrangement off the *si* pathway and onto the *ar* pathway. It is reached by rotation around the C2–C3 bond that brings the terminal methylene further from the allyl group (Figure 8). A *gauche*-out diradical intermediate, **17**, that is 2.9 kcal/mol lower in energy than transition state **16** has also been located on this surface. Rotation around the C3–C4 bond, which is responsible for the inversion of configuration at C4 on the *si* pathway, continues in the same direction on the *ar* pathway. When intermediate **17** is reached, a 360° rotation has occurred. This results in retention of configuration at C4. Rotation around the C1–C2 bond brings the methylene radical in close proximity to the allyl radical and closure to form cyclohexene occurs, possibly through concerted transition state **13**.

A fragmentation pathway out of the diradical caldera was also found for *syn*-vinylcyclobutane (Figure 9). The C2–C3 bond rotation that links diradical intermediate **11** with antarafacial transition state **16** also provides a path to the *cis* fragmentation transition state **18**. Transition state **18** is found to be 0.1 kcal/mol higher in energy than antarafacial transition state, **16**, and 1.1 kcal/mol higher than closure transition state **12**. The *cis* fragmentation process is predicted to be endothermic by 9.7 kcal/mol, and therefore not favorable at low temperatures. The process is, however, entropically favored and likely to proceed at elevated temperatures.

In 1978, Pottinger used kinetic data gathered over a temperature range of 570–670 K to experimentally determine ΔH^\ddagger for both the fragmentation of vinylcyclobutane to butadiene and ethylene as well as rearrangement to cyclohexene. The barriers were found to be 50.2–50.7 and 48.2–48.6 kcal/mol, respectively.²⁷ More recently, Lewis et al. have performed similar kinetic experiments over a broader temperature range of 577–1054 K in order to determine rate constants for the same processes. The observed kinetic data revealed an energy barrier of 49.8 ± 0.4 kcal/mol for fragmentation of vinylcyclobutane and 47.5 ± 0.5 kcal/mol for rearrangement to cyclohexene.²⁸ These values are close to the calculated CASPT2(6,6)/6-31G*//

(26) Lewis, D. K.; Glenar, D. A.; Hughes, S.; Kalra, B. L.; Schlier, J.; Shukla, R.; Baldwin, J. E. *J. Am. Chem. Soc.* **2001**, *123*, 996–997.

(27) Pottinger, R.; Frey, H. M. *J. Chem. Soc., Faraday Trans. 1* **1978**, *74*, 1827–1833.

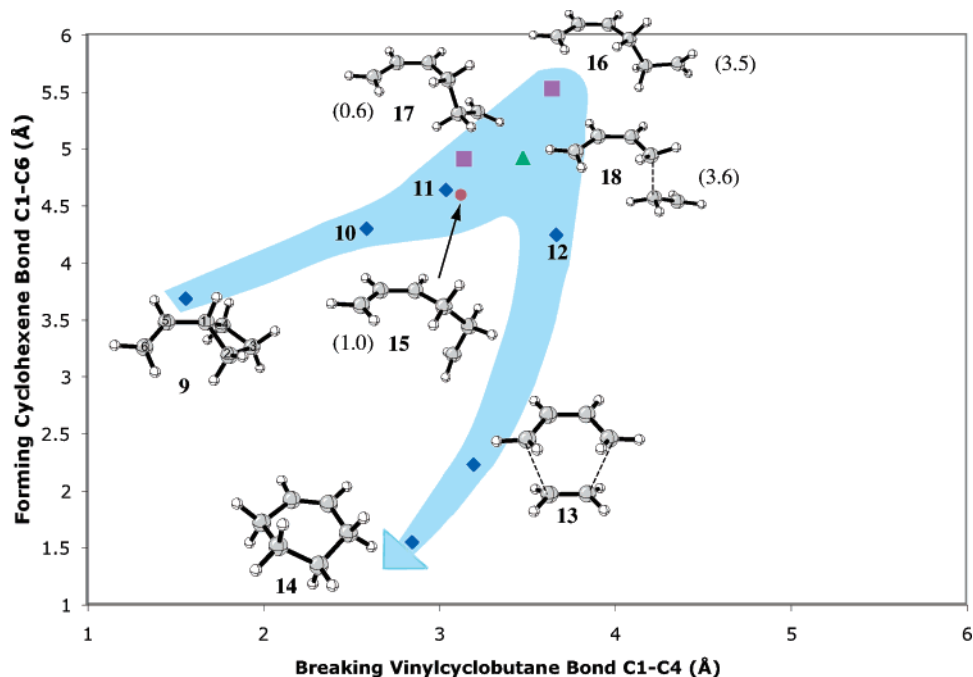


FIGURE 6. Reaction coordinate for the *syn*-vinylcyclobutane rearrangement plotted versus the lengths of the breaking cyclobutane bond and the forming cyclohexene bond. Colored symbols indicate the reaction path through various stationary points: blue diamond = *si* rearrangement, magenta square = *ar* rearrangement, orange circle = transition state for the *sr* rearrangement, green triangle = fragmentation to *cis*-butadiene plus ethylene. Relative energies of structures **15**–**18** with respect to *cis* diradical intermediate **11** are shown in parentheses (kcal/mol).

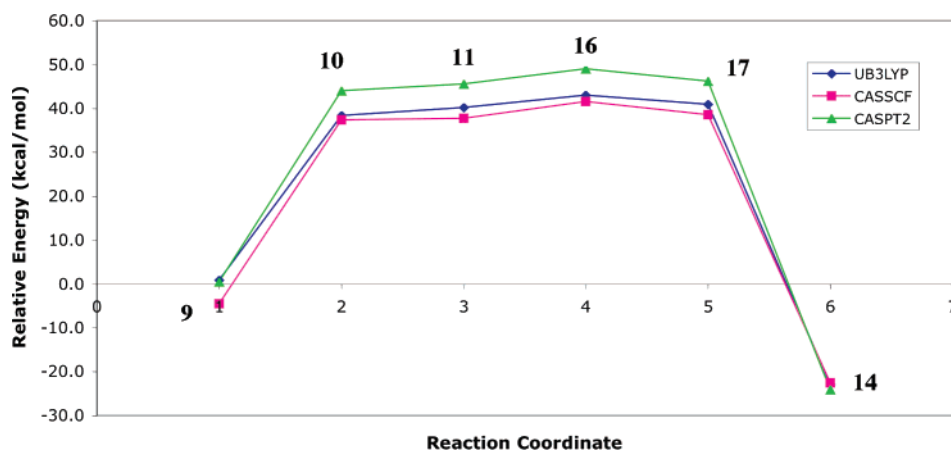


FIGURE 7. Relative energies of stationary points on the *ar* rearrangement of *syn*-vinylcyclobutane.

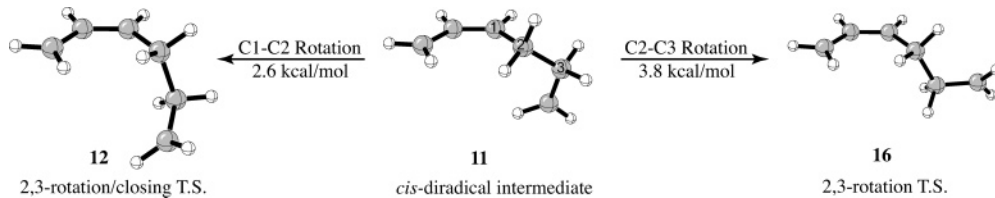


FIGURE 8. Comparison of bond rotations that distinguish the *si* and *ar* rearrangement pathways.

UB3LYP/6-31G* values of 46.1 and 48.1 kcal/mol at 298 K. When scaled to 600 K these barriers increase slightly to 46.8 and 48.7 kcal/mol, respectively. UB3LYP/6-31G* calculations at 600 K predict barriers of 39.4 and 42.4 kcal/mol, underestimating the two barriers by 10.4 and 5.1 kcal/mol, respectively

(28) Lewis, D. K.; Charney, D. J.; Kalra, B. L.; Plate, A.-M.; Woodward, M. H.; Cianciosi, S. J.; Baldwin, J. E. *J. Phys. Chem. A* **1997**, *101*, 4097–4102.

(Figure 10). However, although CASPT2(6,6)/6-31G*//UB3LYP/6-31G* calculations are closest to experimental values, they wrongly predict the barrier for rearrangement to be higher than that for fragmentation of *anti*-vinylcyclobutane. Interestingly, the computed barrier for fragmentation via the *cis* fragmentation pathway, 49.2 kcal/mol, is in better agreement with the experimental value and correctly predicts the fragmentation process to be higher in energy than rearrangement. Experimental

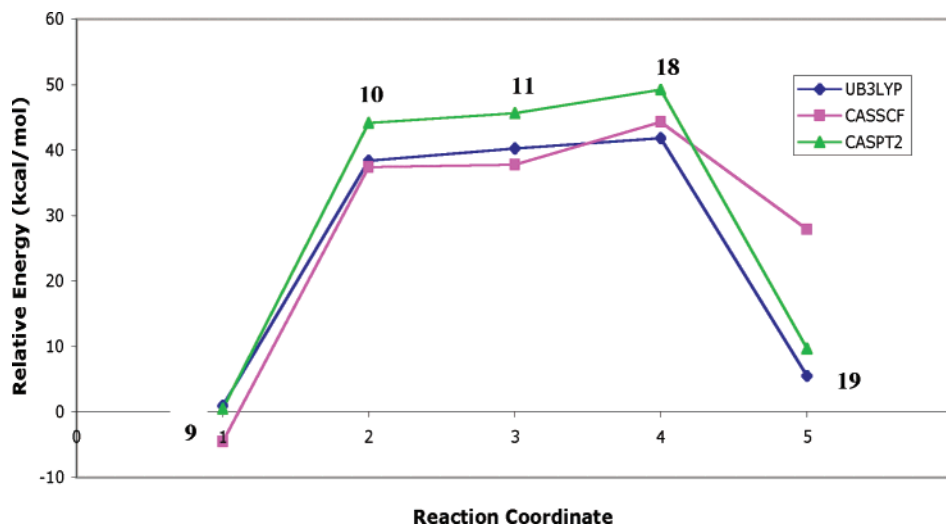


FIGURE 9. Relative energies of stationary points on the fragmentation pathway of *syn*-vinylcyclobutane.

$\Delta H_{570-670\text{ K}}^\ddagger$ (experimental)	50.2-50.7	48.2-48.6
$\Delta H_{577-1054\text{ K}}^\ddagger$ (experimental)	49.8 ± 0.4	47.5 ± 0.5
$\Delta H_{600\text{ K}}^\ddagger$ (CASPT2(6,6)/6-31G**//UB3LYP/6-31G*)	46.8	42.4
$\Delta H_{600\text{ K}}^\ddagger$ (UB3LYP/6-31G*)	39.4	48.7
$\Delta\Delta H_{298\text{ K}}^\circ$ (experimental)	14.8 ± 0.6	-24.9
$\Delta\Delta H_{298\text{ K}}^\circ$ (CASPT2(6,6)/6-31G**//UB3LYP/6-31G*)	6.1	-24.1
$\Delta\Delta H_{298\text{ K}}^\circ$ (UB3LYP/6-31G*)	1.6	-22.9
$\Delta\Delta H_{298\text{ K}}^\circ$ (CBS-QB3)	15.7	

FIGURE 10. Comparison of experimental and calculated energy barriers at elevated temperatures, as well as reaction enthalpies at room temperature.

gas phase ΔH_f° values for vinylcyclobutane and cyclohexene of 23.7 and -1.2 kcal/mol, respectively, indicate a $\Delta H_{\text{rxn}}^\circ$ of -24.9 kcal/mol for the rearrangement of vinylcyclobutane to cyclohexene.^{28,29} This agrees well with the value of -24.1 calculated by CASPT2(6,6)/6-31G**//UB3LYP/6-31G*. The UB3LYP/6-31G* and CASSCF(6,6)/6-31G* values of -22.9 and -22.5 kcal/mol, respectively, are also reasonably close (Table 3 and Figure 10).

The close agreement of CASPT2(6,6)/6-31G**//UB3LYP/6-31G* calculations with experimental barriers for the rearrangement of vinylcyclobutane to cyclohexene is in accord with the satisfactory energetics found at this level for other diradical potential surfaces.^{2,10,12,14} These results are similar to those of the experimental and theoretical studies of the rearrangements of bicyclo[3.2.0]hept-2-ene to norbornene and of vinylcyclo-

propane to cyclopentene.^{2,6,12,14} Both of these rearrangements have been shown to proceed via diradical intermediates and result in a stereochemical mixture of products dictated by the movements of diradical species on flat potential surfaces. Beno et al. and Wilsey et al.¹² explored the rearrangements of bicyclo[3.2.0]hept-2-ene, and Davidson and Gajewski^{14a} and Nendel et al.^{14b-d} studied vinylcyclopropane computationally. All found close agreement between experimental and UB3LYP/6-31G* calculated activation energies. ΔH^\ddagger for bicyclo[3.2.0]hept-2-ene has been reported to be around 49.0 kcal/mol⁶ and calculated to be 50.5 kcal/mol^{12a} while ΔH^\ddagger for vinylcyclopropane has been reported by Wellington to be 49.7 kcal/mol³⁰ and calculated to be 46.9 kcal/mol.¹⁴ This work has shown UB3LYP/6-31G* to be in close agreement with experimental values, while CASPT2(6,6)/6-31G**//UB3LYP/6-31G* calculations are in very good agreement with experiment. As in previous studies, the shapes

(29) Pedley, J. B.; Naylor, R. D.; Kirby, S. P. *Thermodynamic Data of Organic Compounds*, 2nd ed.; Chapman and Hall: London, 1986.

(30) Wellington, C. A. *J. Phys. Chem.* **1962**, *66*, 1671–1674.

of calculated UB3LYP/6-31G* potential surfaces for fragmentation and both rearrangement pathways, *si* and *ar*, are qualitatively very close to those of CASPT2(6,6)/6-31G*//UB3LYP/6-31G* calculations. This indicates that although CASPT2(6,6)/6-31G* single points are in better agreement with experimental values for these processes, relatively inexpensive UB3LYP/6-31G* optimizations provide a good description of the general shape of the diradical potential landscape.

Carpenter,¹³ Doubleday,^{14b,15} and Suhrada¹⁶ have shown that the dynamics of bond rotations on flat potential energy surfaces have significant influence on product distributions. The initial trajectories of bond rotations, rather than the total available energy, have the greatest effect on product distribution. Lifetimes of intermediates are on the order of molecular vibrations. In other words, bond cleavage and bond formation occur faster than the time required for redistribution of kinetic energy through vibrational modes resulting in no equilibration of intermediate structures. These intermediate structures exist on flat potential surfaces with no minima greater than RT and are, therefore, fundamentally different from traditional intermediate structures that are true minima along a reaction pathway. For this reason it may be more appropriate to think of them as “para-intermediates”, as they are similar to but different than traditional intermediates. Doubleday has used quasiclassical dynamics to show that, in the case of the vinylcyclopropane rearrangement, about 80% of the reaction is complete within the first 400 fs.¹⁵ A similar study of the quadruply degenerate bicyclo[3.1.0]hex-2-ene rearrangement has shown that most of the starting 4-*exo-d*-bicyclo[3.1.0]hex-2-ene rearranges within the time frame of only one molecular vibration. This dynamic matching^{13b,c} helps explain the nonstatistical stereochemical mixture of products obtained from [1,3] sigmatropic shifts such as the vinylcyclobutane to cyclohexene rearrangement.

Conclusion

Computational studies of the vinylcyclobutane–cyclohexene rearrangement show that the mechanism proceeds via short-

lived diradical species moving across a caldera. The favored pathway for rearrangement is suprafacial with inversion of configuration at C4, but additional stationary points on the computed potential energy surface are only slightly higher in energy than the lowest energy *si* pathway. The potential energy surface for rearrangement may merge with that of the Diels–Alder reaction between butadiene and ethylene just prior to cyclohexene formation. Deviations from the *si* path via these higher energy stationary points explain the experimentally observed stereochemical mix of products. The mixture of products is not purely random even though the rearrangement proceeds via diradical species. A small preference for the Woodward–Hoffmann “allowed” products is due to orbital interactions that govern the vinylcyclobutane ring opening, but not to an aromatic transition state of a conventional concerted pericyclic process. These orbital interactions and the dynamic motions of diradical species moving along the flat potential surface before ring closure govern the observed stereochemical preferences.

Acknowledgment. We are grateful to the National Science Foundation for financial support through a research grant to K.N.H. and an IGERT (MCTP)-DGE-0114443 fellowship to B.H.N. as well as to the National Center for Supercomputing Applications, UCLA’s Office of Academic Computing, and UCLA’s California Nanosystems Institute for computational support. We thank John E. Baldwin and Charles Doubleday for helpful discussions. The cover shows a National Park Service photo by D. E. White.

Supporting Information Available: Cartesian coordinates of all stationary points reported in this manuscript and their absolute energies in hartrees as well as the full author lists for refs 19 and 20. This material is available free of charge via the Internet at <http://pubs.acs.org>.

JO051273L